Key Engineering Materials
ISSN: 1662-9795, Vol. 926, pp 1802-1808
doi:10.4028/p-txh1t4

Submitted: 2021-12-09
Revised: 2022-02-01
Accepted: 2022-02-01
Online: 2022-07-22

Numerical Analyses of Deformation Mechanisms in a Novel Dimensional Calibration Technique for Thin-Walled, Open Extrusions

Xianyan Zhou[a], Jun Ma[b] and Torgeir Welo[c*]

Department of Mechanical and Industrial Engineering, Norwegian University of Science and Technology, 7491 Trondheim, Norway

[a]xianyan.zhou@ntnu.no, [b]jun.ma@ntnu.no, [c*]torgeir.welo@ntnu.no

Keywords: Thin-walled extrusion, dimensional accuracy, dimensional calibration, deformation mechanism

Abstract. High dimensional accuracy is of crucial importance in digital manufacturing to guarantee production capability and product performance. For manufacturing of thin-walled complex extrusions, it is often challenging to meet the tight dimensional tolerance requirements for automated mass production, due to dimensional imperfections and variations accumulated from the thermo-mechanical processing history. Recently, a new calibration technique, called Transverse Stretch and Local Bending, was developed, enabling significant improvement of the dimensional accuracy of thin-walled open profiles at a low cost. However, the deformation mechanisms have not been well understood, which in turn affect the process design for achieving high-precision products. In this study, a through-process finite element model was established and experimentally verified, which is used as a tool to investigate the mechanisms in the calibration process. It is found that the gap opening is mainly reduced in the inserting stage, but the calibration stage plays a key role in achieving high-precision products after unloading. The critical factor to achieve high dimensional accuracy is reducing the through-thickness gradients on both the profile bottom and sidewall. By controlling the total vertical displacement in transverse stretch and local bending, the stress gradients can be effectively reduced, and the dimensional deviation caused by springback after unloading can be well mitigated. This fundamental study will benefit the industry to obtain high-precision extrusions.

Introduction

The declaration of rapidly accelerating the transition to 100% zero-emission sales of new cars and vans has been agreed by many countries, see e.g. COP26 [1]. Expanding the use of electric vehicles (EVs) is a key to realizing this declaration [2]. Aluminum extrusions are attractive for use in EVs due to many advantages such as lightweight, high energy absorbing capability and sustainability [3], [4]. For example, extrusions are highly favored in manufacturing of EV battery trays and enclosures [5]. However, many critical dimensional problems are associated with thin-walled extrusions, including gap opening, twisting, sidewall inclination and local convex, etc. [6]. These defects severely impede the development of thin-walled products in digital mass manufacturing, as tight dimensional accuracy of products is required [7]. Thus, it is of great importance to developing effective and cost-efficient techniques to improve the dimensional accuracy of aluminum extrusions to meet strict industrial requirements.

Up to now, many calibration techniques have been developed and applied in industries addressing the dimension defects in various applications. Some simple and industrially used calibration techniques include stretching [8] and ironing [9], etc. Nevertheless, these techniques can only be applied to specific simple geometries but not for complex geometries, such as open profiles with various thicknesses. Hydraulic calibrations ensure high dimensional accuracy, but the production efficiency is still limited [10]–[12]. Thermal calibration is attractive to reshape hard-to-deform materials, but the cycle time and cost are high [13], [14]. Therefore, new calibration techniques, ones that efficiently and economically enable improved dimensional accuracy of complex thin-walled profiles, are urgently required to meet the market demand.

Recently, a new mechanical calibration technique, named transverse stretch and local bending (TSLB), was proposed. It combines the mechanisms of stretching and bending, enabling high

dimensional accuracy to a low-cost penalty [15]. The feasibility of this technique was assessed experimentally with complex U-shape extrusions [15]. The deformation mechanisms of stretching and bending were studied by finite element analysis (FEA) [6]. Also, the die geometry was investigated and optimized, which shows a significant influence on the stress-strain evolutions and the improvement of dimension accuracy. Springback, as one critical issue in sheet metal forming, has not been studied in detail as to how the stress and strain distribution in the calibration affects the subsequent springback. Thus, to achieve high dimensional accuracy, it is important to clarify the mechanism that contributes to mitigating springback and variability.

In this study, the TSLB test with a thin-wall, open extrusion will be conducted to validate the accuracy of the FEA model. The mechanisms and stress evolution in this technique will be revealed with FEA. Its effects on the subsequent springback and the global dimensional accuracy will be clarified.

Methodology

In this study, both experiments and numerical simulations were conducted to understand the deformation mechanisms in the TSLB process. A TSLB setup was designed, and the tests were conducted to study the feasibility of this technique. An FEA model of the TSLB process was established. Based on this model, the effects of the initial dimensions of the profiles (sidewall angle and bottom angle) on dimensional accuracy (gap opening) of final profiles were revealed.

Experiments

Material description. A batch of AA6082-T4 aluminum extrusions provided by Benteler Automotive Raufoss were used in this study. A typical sample is shown in Fig. 1(a). The cross section is in a U-shape with varying thicknesses. The gap opening G_A, as shown in Fig. 1(b), is applied to characterize the springback levels, the deviation of which mainly results from two factors, the large sidewall angle θ_1 and the bottom angle θ_2.

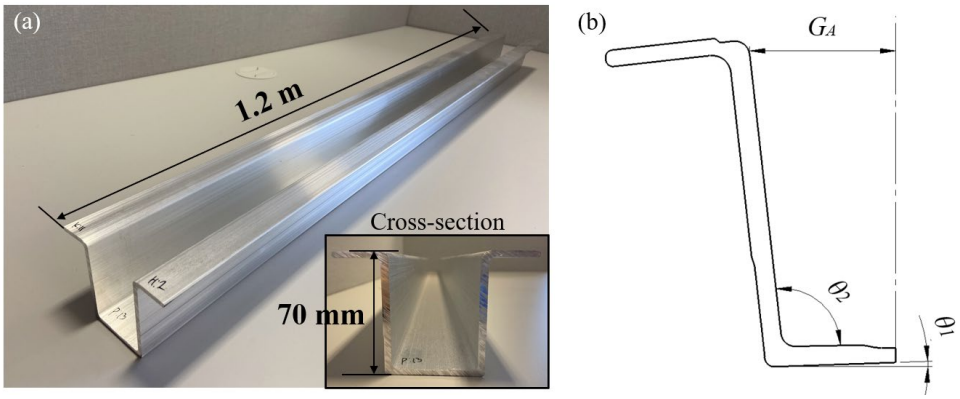

Fig. 1 Description of as-received samples: (a) overview of one typical sample and (b) definition of the geometric parameters (G_A: top gap opening; θ_1 and θ_2: bottom and sidewall angles, respectively).

Uniaxial tensile tests were conducted to investigate the mechanical properties of the as-received materials. The samples were taken with three orientations (0°, 45°, and 90° relative to the extrusion direction). The average values of the stress-strain data along different directions were used to describe the material behaviors in FEA. More details about the uniaxial tensile test can be found in previous work [15].

Experimental setup. The setup of the TSLB process is shown in Fig. 2. The wedge is driven up and down by the hydraulic system. The shim blocks between the profile and wedge are driven toward the interior walls of the profile, which pushes them up against exterior inserts that are fixed on the

base plate. Under the action of the shim blocks and inserts, the profile is formed to the geometry made up by the inserts and the upper tool on the outside and the shim block on the inside.

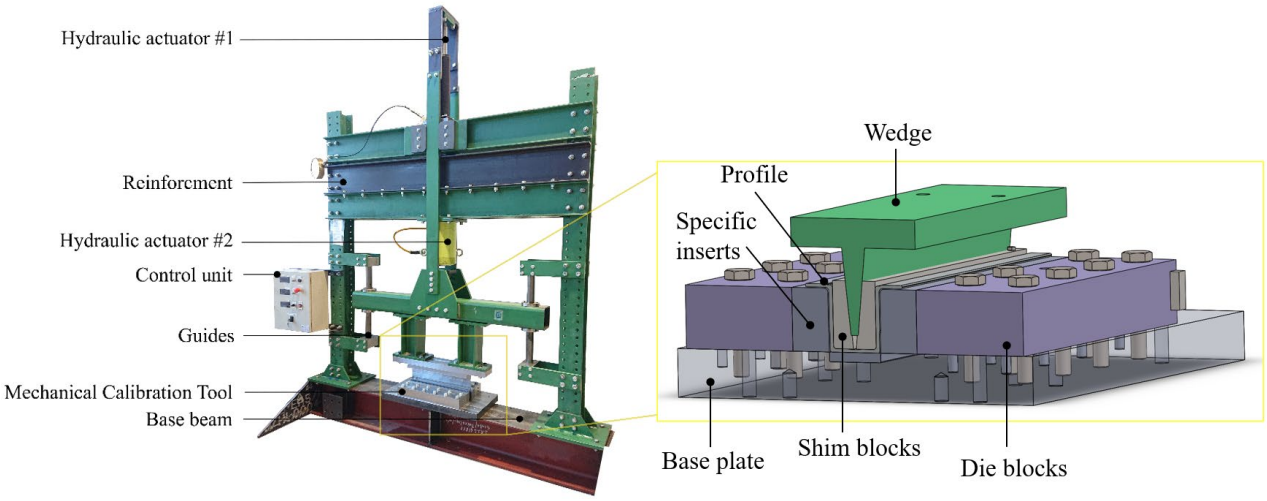

Fig. 2 Configuration of the experimental setup (redrawn from [15]).

Experimental procedure. The TSLB process contains the following steps: (1) the profile is put on top of the two side inserts. For better observing the calibration capability, the profile was initially opened to obtain high initial gap opening values; (2) one big block is applied to push the profile to the die bottom; (3) the big block is removed, and the shim blocks are applied. Driven by the wedge, the shim blocks force the profile to move toward the inserts till the force on the wedge reaches a pre-set value; and (4) the wedge, the shim blocks and the profiles are sequentially retracted from the machine. Before and after calibration, the dimensions of the sample were measured in a 3D-measurement machine, Leitz PMM-C 600 coordinate measuring machine (CMM). More details of the measurement strategy can be found in previous work [15]. The geometric data on the middle cross section of the profile was defined to verify the accuracy of the FE model.

Finite element model and virtual experimental plan

A 2D TSLB FE model was established in Abaqus 2017, as shown in Fig. 3. Only half the geometry was modelled due to symmetry. It consists of the wedge, shim block, profile and die block. The wedge and die are assumed as rigid bodies, and the profile is set as deformable. The shim block is also set as deformable due to the potential stress concentration during the calibration stage. The elastic modulus and true plastic stress-strain curve obtained from uniaxial tensile tests were used to describe the elastoplastic behavior of the aluminum profile. The mechanical properties of carbon steel were employed to simulate the elastic deformation of the shim block. Surface-to-surface contact together with a Coulomb friction model with a coefficient of 0.2 was used to describe the friction behavior between different contact surfaces.

The die is completely fixed, and the symmetry boundary was set on the bottom middle cross section of the profile. Two steps were represented to simulate the entire TSLB process. In the first step, both the shim block and the wedge move downward till the profile contacts the die bottom. In the second step, the shim block is set free, and the wedge continues moving downward till the block fully contacts the die. Both steps are set as dynamic explicit.

Another static implicit model was built to simulate the springback behavior, as an indication on the effect of stress state prior to unloading. In this model, only the profile was left with the x-symmetry boundary on the profile symmetrical line, and the freedom of the bottom node on that line was constrained along y-direction. The deformation information after the calibration was transferred to the springback model by defining the initial state of the profile.

One simulation was initially run to validate the accuracy of the model and study the deformation mechanisms as to how the stress state prior to unloading affects the subsequent springback levels.

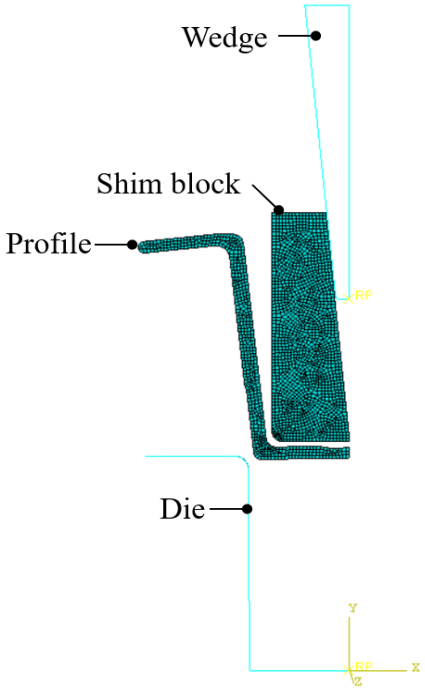

Fig. 3 Configuration of TSLB FE model.

This is labeled as the Ref case in the following analysis. The total vertical displacement of the wedge in the Ref case was measured to be 97.8 mm. The other two cases with different vertical displacements (91.8 mm and 101.8 mm) were analyzed for a better understanding of the mechanisms for improving dimensional accuracy. They are named Case 1 and 2.

Results and Discussion

Validation of finite element model. Fig. 4 compares the profile's final dimensions achieved from the TSLB experiments and simulations. Six points on the profile's inner wall of the profile were examined, labeled as N1-N6. They are evenly distributed along the vertical direction with an interval of 10 mm. The nominal dimension from the inner wall to the middle line of the profile is 25.10 mm. The top gap opening of the as-received profile is as high as 31.20 mm and reduced to 25.47 mm after calibration; only 0.37 mm deviated from the nominal value. The simulated dimensions on the 6 points are slightly different from the experimental ones. The deviation between experiments and simulations is within 0.14 mm—only 0.56% off the nominal value. Thus, this model can provide high accuracy (99.44%) in analyzing the TSLB process.

Deformation mechanisms. Fig. 5 presents the von Mises stress evolution on the profile's cross-section during the TSLB process. Initially, the parts including wedge, shim block, profile, and die are located as shown in Fig. 5(a). Then, the block and the wedge move down and push the profile to the bottom of the die. The gap opening is greatly reduced at the end of the inserting stage (Fig. 5(b)). However, the stress state can cause high springback after unloading. Thus, the calibration stage is applied. As shown in Fig. 5 (c), the wedge further pushes the block to move downward and sideward simultaneously, and accordingly the block forces the profile to move towards both the die wall and bottom. The geometry of the profile coincides with the designed dimensions. After calibration, a high stress state can be observed in the areas around the profile corner. In the entire forming process, without proper control of the stress distribution, high springback would expectedly occur after unloading. Thanks to this stress distribution induced in the calibration stage, only slight springback occurs so that no evident dimensional deviation was observed, as shown in Fig. 5(d). The gap opening is increased by only 0.02 mm from 25.26 to 25.28 mm during the springback stage.

To further investigate the stress distribution on the areas around the profile corner prior to springback, the stress components in the three cases with different moving displacements of the wedge were comparatively analyzed, as shown in Fig. 6. In Case 1 with a moving displacement of 91.8 mm, there are large red regions, as shown in Fig. 6 (a1) and (a2), showing a high tensile stress state in both the bottom (along x direction) and the sidewall (along y direction). It also can be found that the sidewall near the profile corner (interest area B) is slightly bent after calibration. Moreover, significant stress gradients through the thickness are observed in the interested regions A and B, and the stress difference between the outside and inside can be up to about 60 MPa (from -180 to 240 MPa). Such a stress gradient through the thickness around the profile corner is expected to induce significant springback after unloading. With the increase of vertical displacement of the wedge to the Ref Case, both the bottom and the sidewall the profile is further compressed along the thickness direction, as shown in Fig. 6 (b1) and (b2). Due to the compression, the red regions turn to be green and the through-thickness stress gradients in both the bottom and the sidewall are significantly

weakened. This implies that the springback after unloading will become much smaller, as compared to Case 1.

In Fig. 6 (c1) and (c2), a higher moving displacement induce more compression through the thickness, which provides the bottom and the sidewall with a more uniform stress state not only in thickness direction but also in the longitudinal direction. As the stress gradients almost disappear, springback will be effectively controlled. It should be noted that the curved area in Case 1 is completely flattened in Case 2, thus providing higher dimensional accuracy in the corner zone.

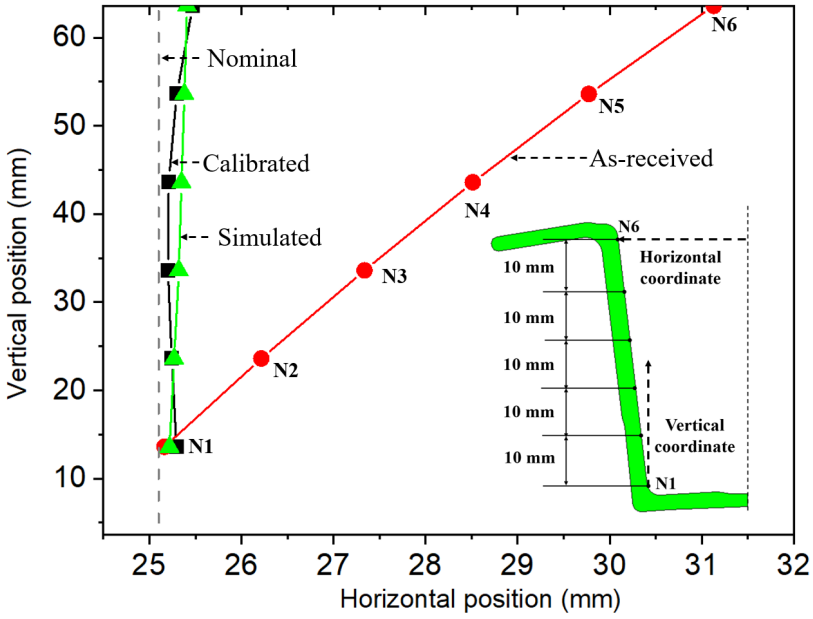

Fig. 4 Comparison of experimental and simulated final profile dimensions on 6 points.

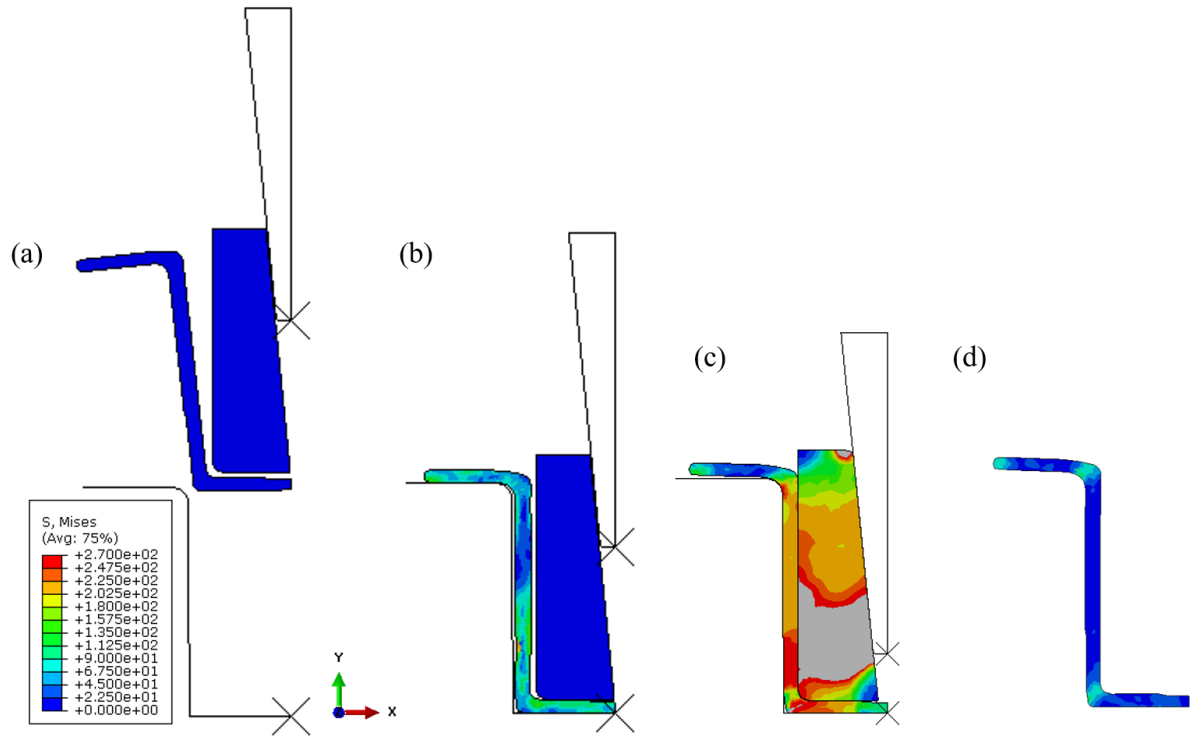

Fig. 5 Evolution of von Mises stress during the TSLB process: (a) initial stage; (b) end of inserting; (c) end of calibration stage and (d) after springback.

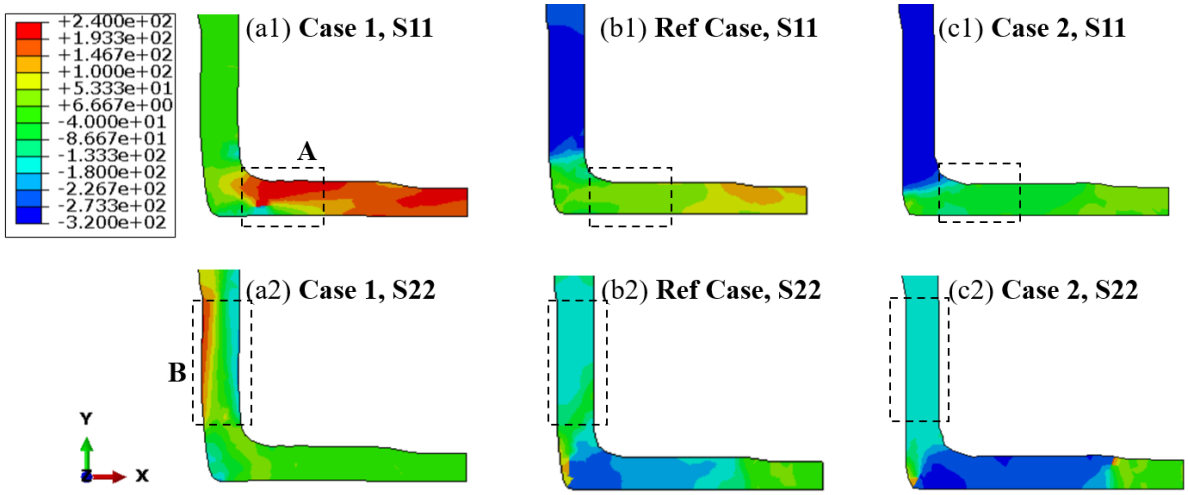

Fig. 6 Distribution of stress components on the profile of interest at the end of calibration stage: (a1) S11 and (a2) S22 in Case 1; (b1) S11 and (b2) S22 in Ref Case and (c1) S11 and (c2) S22 in Case 2 (unit: MPa).

Furthermore, the dimension deviation caused by the springback in Case 1, Ref Case and Case 2 were examined as 1.90, 0.02 and 0.03 mm, respectively. The dimension deviation is significantly reduced to a very low level (about zero) by increasing the total vertical displacement of the wedge.

The reason is that the strong stress gradient in the thickness direction under small thickness compression generates a high bending moment in the bottom/sidewall areas around the profile corner, which would cause significant springback after unloading. However, under a high level of thickness compression by increasing vertical displacement of the wedge, the through-thickness stress gradient can be dramatically weakened or even eliminated. Thus, the springback induced dimensional deviation can be well controlled by proactively regulating the stress distribution on the formed profile in the TSLB process. Note that it is not suggested to apply an over-large thickness compression, as severe compression may cause the wall thickness reduction, the deformation of the shim block as well as higher requirements on the machine capacity. Therefore, for industrial application of the TSLB technique, the tooling geometries, process routes and parameters need to be further optimized for improving the dimensional accuracy of products and reducing the manufacturing investment.

Conclusion

This research aims to provide an in-depth insight into the deformation mechanisms in a novel TSBL technique for improving the springback affected dimensional accuracy of formed products. The TSBL test was conducted, and an accurate FEA model was established. The deformation mechanism was investigated by analysing the stress distribution caused by the TSBL method. By comparing the stress distributions and springback levels, the critical factor for achieving high dimensional accuracy was identified. The following conclusions can be made:

1. A 2D TSBL FE model including calibration and springback stages was built and verified by experiments. The gap opening is significantly reduced during the inserting stage. The calibration further improves the dimensional accuracy and generates the specific stress distribution, which can mitigate the subsequent springback after unloading.
2. The springback induced dimensional deviation can be well controlled by tailoring the stress distribution on the formed profile in calibration. Reducing the through-thickness stress gradient on the bottom/sidewall areas around the profile corner is the key to controlling springback for improved dimensional accuracy.
3. The through-thickness stress gradient on the profile can be reduced by increasing the vertical displacement of the wedge in the TSBL process. The compression deformation to the profile thickness should be carefully controlled to provide the bottom/sidewall with a relative uniform stress state but avoid severe reduction of the profile thickness.

Acknowledgments

Massive thanks are given to Hydro and Benteler and RCN under the grant of Expect (grant no. 321571) for the financial support. Sincere gratitude is given to PhD student William Matthew Williams for paper reviewing and language proofing.

References

[1] Information on https://www.gov.uk/government/publications/cop26-declaration-zero-emission-cars-and-vans/cop26-declaration-on-accelerating-the-transition-to-100-zero-emission-cars-and-vans.

[2] A. Ghosh, Possibilities and challenges for the inclusion of the electric vehicle (EV) to reduce the carbon footprint in the transport sector: A review, Energies. 13 (2020).

[3] K. Zheng, D. J. Politis, L. Wang, and J. Lin, A review on forming techniques for manufacturing lightweight complex—shaped aluminium panel components, Int. J. Light. Mater. Manuf. 1 (2018) 55–80.

[4] K. Wang et al., High-efficiency forming processes for complex thin-walled titanium alloys components: State-of-the-art and perspectives, Int. J. Extrem. Manuf., 2 (2020) 032001.

[5] Information on https://www.hydro.com/en-NO/aluminium/industries/automotive/electric-vehicles/.

[6] X. Zhou, T. Welo, J. Ma, and S. A. Tronvoll, Deformation Characteristics in a Stretch-Based Dimensional Correction Method for Open, Thin-Walled Extrusions, Metal. 11 (2021) 1786.

[7] Aluminium extruders council, Aluminium extrusion manual. 2018.

[8] W. Zhou, Z. Shao, J. Yu, and J. Lin, Advances and trends in forming curved extrusion profiles, Materials (Basel)., 14 (2021) 1603.

[9] Information on https://thelibraryofmanufacturing.com/ironing.html.

[10] C. Bell, J. Corney, N. Zuelli, and D. Savings, A state of the art review of hydroforming technology: Its applications, research areas, history, and future in manufacturing, Int. J. Mater. Form. 13 (2020) 789–828.

[11] L. H. Lang, S. J. Yaan, Z. R. Wang, X. S. Wang, J. Danckert, and K. B. Nielsen, Experimental and numerical investigation into useful wrinkling during aluminium alloy internal high-pressure forming, Proc. Inst. Mech. Eng. Part B J. Eng. Manuf. 218 (2004) 43–49.

[12] J. P. Abrantes, A. Szabo-Ponce, and G. F. Batalha, Experimental and numerical simulation of tube hydroforming (THF), J. Mater. Process. Technol. 164–165 (2005) 1140–1147.

[13] R. Neugebauer, T. Altan, M. Geiger, M. Kleiner, and A. Sterzing, Sheet metal forming at elevated temperatures, CIRP Ann. - Manuf. Technol., 55 (2006) 793–816.

[14] Information on https://www.twi-global.com/technical-knowledge/job-knowledge/distortion-corrective-techniques-037.

[15] C. A. Raknes, J. Ma, T. Welo, and F. Paulsen, A new mechanical calibration strategy for U-channel extrusions, Int. J. Adv. Manuf. Technol. 110 (2020) 241–253.